Agnieszka LISOWSKA-LIS
PAŃSTWOWA WYŻSZA SZKOŁA ZAWODOWA W TARNOWIE
Mickiewicza 8, 33-100 Tarnow, Poland

Thermographic and Electrical Test of Medium Voltage Surge Arresters

Abstract

The paper presents the results of a thermal test (conducted with thermographic camera, coupled with an electrical test) of medium voltage metal–oxide surge arresters. Surge arresters (for U_c=18 kV) were tested for the leakage current and surface temperature: for 5 minutes under state 50 Hz alternating voltage 18 kV. The surface temperature of the MOAs correlates with an increase in leakage current. The result shows that the 0.6 mA AC leakage current in the medium voltage metal–oxide surge arrester (18 kV) is above the stable operating point, and the loss of electrical power is higher than the effective heat dissipation in the arrester. After 5 minutes of high voltage impact U = 18 kV, the surface temperature of the surge arrester was (4.32±0.55) K higher than the initial temperature. The IR camera can be used to detect the faults of ZnO metal–oxide surge arresters that lead to an increase in surface temperature.

Keywords: surge arresters, medium voltage, thermography, discharge current, cooling.

1. Introduction

Temperature measurement and early detection of local increase in the surface temperature may be crucial for the power system machinery and equipment as indication of failure or its improper work. Thermal cameras used for monitoring of the equipment can easily detect increase of the surface temperature of electrical equipment [1, 2, 3, 4].

Surge arresters are very efficient equipment applied for protection of high voltage and medium voltage electrical equipment. They are used to eliminate the effect of overvoltage caused by incoming surges. They are widely used not only to protect especially transformers in the distribution systems but also to protect circuit- breakers, bushings, lines. Effective overvoltage protection prevents the damage from lightning strike, electrostatic discharge, electromagnetic pulse (usually accompanying the lightning strike). It also stops the current from the surge caused by switching operation in the power system discharge. The current from the surge is diverted through the arrester (usually to the ground). Effective overvoltage protection requires different surge arrester types to be used [5, 6, 7].

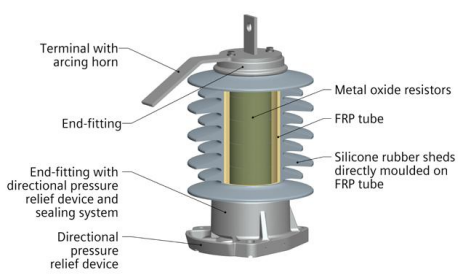

Fig. 1. Construction of metal-oxide surge arrester [7]

Metal–oxide varistors have been used since the 1970s to limit surges in electrical network. They are also known as gapless arresters and variable-resistors (var+istors). **V**aristors are manufactured on the basics of polycrystalline ZnO (about 90%) with additives of magnesium-, bismuth-, cobalt- and chromium-oxides. In the medium voltage surge arrester (Fig 1.) varistors (pastilles stack) are covered in fiber-reinforced plastic tube, and the silicone rubber sheds are directly molded on them to avoid moisture ingress, gaps between the layers or inclusions.

The proper varistors functional parameters may be achieved due to the physical and chemical properties of metal- oxides (transmitting electromagnetic waves, thus IR waves), as well as the technological process of varistors production. The most important is the strongly nonlinear current–voltage characteristics: $I=C\cdot V^a$, (I - current, V - voltage, C, a - constants) [6, 7]. The microscopic structure of the varistors shows the presence of polycrystalline grains slightly different in shape and sizes. The homogeneity of that structure is crucial for the proper parameters of the varistor. The total varistors current is the sum of the partial discharge currents flowing through inter-grain junctions [8]. Nonlinear varistor current-voltage characteristic normalized by the varistor geometry to $E = f(J)$ plot presenting the electric field E vs. the current density J is presented in Fig. 2 [5].

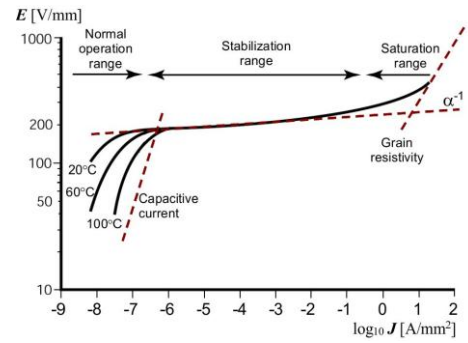

Fig. 2. Characteristic of metal-oxide varistor as electric field vs. current density E= f(J), [5]

In the first range (normal operation) the energy dissipated in the varistor is small, due to very small values of leakage current (due to varistor capacitance). Varistor resistance is maximal. The leakage current strongly depends on varistor temperature [8, 9]. The surface temperature changes in time correlate with the energy generated inside the elements, thus it can be numerically analysed and modelled [10, 11, 12, 13]. In the continuous operation, the arrester operates in the leakage current region on the voltage vs. current curve. In the case of the operating duty, i.e., during a lightning or switching energy impulse, the discharge current flows. The arrester limits the voltage to the residual voltage level (U_{res}). The measurement of the reference voltage U_r (at the reference current) and residual voltage (at the nominal discharge current) ensures a control of the $U=f(I)$ characteristic of surge arrester. They are done by producers as quality tests [6]. The temperature dependence of the arrester conductivity is negligible. [8]. In the other case the construction of the surge arrester as presented in Fig. 1, provides mechanical isolation of varistors to protect the fragile polycrystalline elements (in polymer tube housing and silicone rubber outer cover). Those elements of arrester must transmit effectively thermal radiation from varistors (but they are not as efficient as metal radiators). Stabilization process is repetitive and after cooling the arrester may return to the stable operating point (Fig 3). If effective factors on the heat transfer coefficient are considered constant, heat dissipation ability may be approximated as a linear function up to 100°C. In that range the achieved thermal balance diagram shows that the arrester surface temperature vs. thermal power loss characteristics is linear (at constant voltage applied), [11].

If energy is too high it leads to destruction of the varistor micro- or macrostructure and finally to cause saturation of the varistor. As presented in Fig. 3 the current flowing through the varistor

increases so rapidly that varistor does not stabilize the voltage any more. Electrical energy leads to increase in thermal energy generated and rapid destruction of varistor. In the macroscale it may even cause varistor explosion [14].

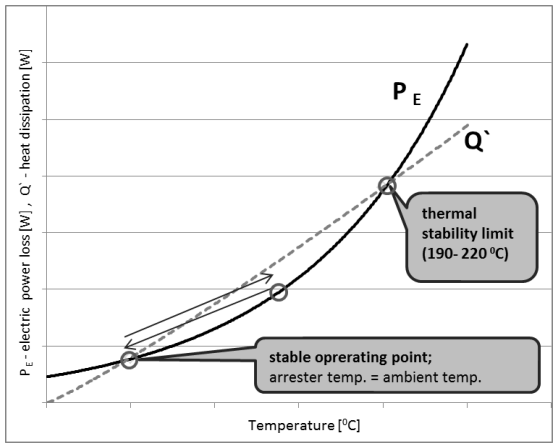

Fig. 3. Characteristic of metal-oxide varistor Q` heat dissipation and P_E vs. Temperature (after [6] and [7])

Varistors are tested before exploitation to confirm stable operational properties (with AC, impulse current, or DC). The producer declares continuous operating voltage U_c (in V), nominal discharge current (for 8/20 μs pulse) I_n (in kA), Voltage protection level U_{pn} (in V), at I_n and maximal partial discharges in pC. Medium voltage surge arresters are usually covered with silicone surface to protect metal oxides from the ambient moisture [5, 6]. That is also important for the surface varistor temperature analysis using thermal cameras. Emissivity coefficient (ε) of the matt silicone rubber is high, about 0.97 [3, 4].

The varistor surface temperature in terms of time T(t) can be calculated as:

$$T(t) = T_a + (T_0 - T_a)\cdot e^{-t/\tau} \quad (1)$$

where: τ is the time constant, T_0 is the initial temperature of varistor, T_a is the ambient temperature. Generally, cooling curve time constant has been calculated with the following equation [12]:

$$\tau = 0.63(T_0 - T_a) \quad (2)$$

The calculations are simplified as the varistor surface initial temperature is the same as the ambient temperature.

Recently some researches were dedicated to analyze arrester surface temperature and leakage current, or state of the arresters. Novizon and Zulkurnain Abdul-Malek (2016) analysed correlation with third harmonic resistive leakage current and condition of ZnO arrester. Some analysis of power loss problems, degradation of varistors and temperature changes were done both in the laboratory and in the field searches [15, 16].

2. Methods

The analysed sample consisted of 21 medium voltage outdoor metal oxide surge arresters MOA. Their nominal parameters are provided in Tab. 1.

Tab. 1. Surge arresters parameters

Parameter	
Continuous operating voltage, U_c	18 kV
Rated voltage U_r (at the leakage current 3 mA)	>20.3 kV
Nominal discharge current, I_n	10 kA
Voltage protection level: U_{pn} (residual voltage) at I_n, V	63 kV
Maximal partial discharges in pC	<5pC
Thermal energy rating W_{th}, kJ/kVr	10 kJ/kVr

The arresters worked outdoors for 3-5 years before the experiment as overvoltage protection equipment. They were used to protect medium voltage distribution transformers.

All of them had been exposed to surges or discharges before. Due to inspection the arresters were in good condition and they had been working properly before.

The surge arresters were disassembled and taken for the laboratory test in high voltage laboratory (laboratory is accredited and certified). Surge arresters were tested with AC/DC test systems produced by F.A.E. Zwarpol Sp. z o. o. These systems are designed to test dielectric strengths with alternating or constant voltage. They consists of high voltage test transformer (type TP), control panel (type PS), voltage divider (DN) and a control transformer (TRP10). Power of the control system ranges up to 100 kVA, maximum high voltage output ranges up to 300 kV (Fig. 4.). Controlling by means of a desktop equipped with a control autotransformer together with a drive operating under the control of a microprocessor controller was applied.

The surge arresters were put under the voltage 18 kV (50 Hz) for 5 minutes. After that time the voltage was switched off and the system was grounded.

Fig. 4. Surge arresters during high voltage laboratory test

During the experiment the voltage U, V, and the AC arrester leakage current I_{arr}, A were registered.

The initial surface temperature of MOAs was close to ambient temperature, ranging from 15 to 20 degrees. The surface temperature T, °C, of the surge arrester was registered using the thermal camera every minute for 10 minutes. After that time temperature of the surface of surge arresters was still monitored until the surface surge arrester temperature reached the ambient temperature (30…90 minutes). In the course of the study more than 1000 thermograms were prepared. Measurements were made using FLIR thermal imaging model E50 (240×180 pixel matrix, resolution 0.05°C at 30°C, image refresh rate 60 Hz). Laboratory conditions during the measurements were as follows: ambient temperature 19°C, RH 60%. Distance to the thermal camera: (0.5…3) m. The thermograms were analysed using FLIR Tools+ 5.2 taking into consideration: air temperature, relative humidity in % (RH), emissivity (ε), distance from the object. The thermograms were analysed for the surface temperature, changes of the temperature in time, the temperature distribution on the area, the detection of anomalies and hot spots on the surface.

After initial research 21 MOA of one type were chosen for statistical analysis (a thermal test made with a thermographic camera, coupled with electrical test). Group A: consisted of 15 MOA – for which leakage current was I_{arr} = 0.3 mA at $U = U_c$ = 18 kV. Group B: consisted of 6 MOA – for which leakage current was I_{arr} = 0.6 mA at $U = U_c$ = 18 kV.

The statistical analysis was performed with the EXCEL MS Office tools. The analysis included arrester surface temperature changes in time $T(t)$; correlation between the surge arrester current and surge arrester surface temperature $R(I_{arr};T)$; the rate of temperature increase ΔT; derivative of temperature over time: dT/dt. Results were statistically tested using one way ANOVA, t test. Statistic differences between groups were determined for α<0.050 and α<0.010. Correlation was analysed in J.Guilford`s scale.

3. Results

Most MOAs under the high voltage at the level of continuous operating voltage ($U = U_c$) presented the proper parameters. In group A, the leakage current I_{arr} did not exceed 0.3 mA at U = 18 kV for 5 minutes. These are normal values. For continuous operating voltage (U_c), the AC leakage current I_{arr} should not exceed 0.3 mA [6, 7]. For group A, changes in surface temperature T vs. time were not significant. It confirms that arresters work at the stable operating point. If the surface temperature is close to the ambient temperature during the experiment, it means that the heat losses compensate for the loss of electric power [6, 8].

In the case of group B the leakage current value I_{arr} was about 0.6 mA. The surface temperature T in group B was increasing during high voltage treatment (Fig. 5). After 5 minutes of high voltage impact U = 18 kV, the surface temperature of the MOAs was (4.32±0.55) K higher than the initial temperature. The linear approximation of the surface temperature shows that the increase in temperature (Medium Value) was about ΔT = 0.51 K for each minute. Increase in temperature was almost the same for the next 5 minutes after the voltage was switched off. Heat dissipation does not compensate for the electric power loss in the varistors inside the MOA [9]. There were statistically significant differences in the surface temperature of the MOA between groups A and B (level of significance α<0.01).

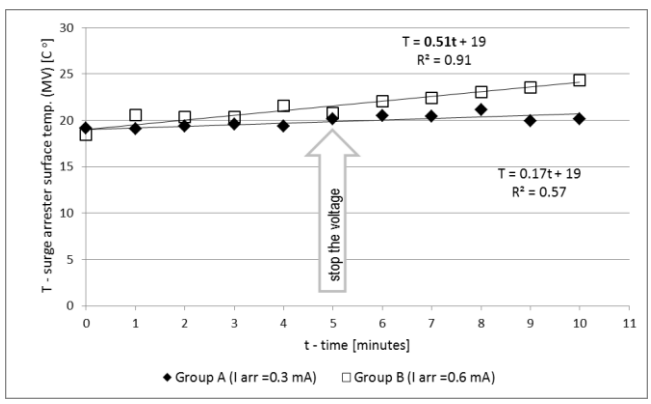

Fig. 5. Characteristic of surge arresters surface temperature (MV – medium value) vs. time

The exemplary thermograms of the surge arrester with higher surface temperature T (group B) are presented in Fig. 6. The highest temperatures on the surface of the arresters (hot spots) were recorded in various areas. Most often, the upper and middle areas.

Fig. 7 presents two MOAs from group B: one before and one after the U=18 kV treatment for 5 minutes. The surface temperature T is higher for the arrester after 5 minutes of treatment. The MOAs in group B are cooled down to ambient temperature for a further (20…30) minutes. The surface temperature correlates with the energy produced in MOA [9, 10, 11, 12].

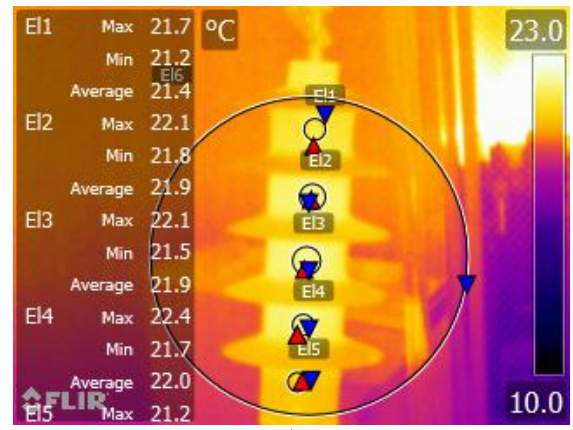

a)

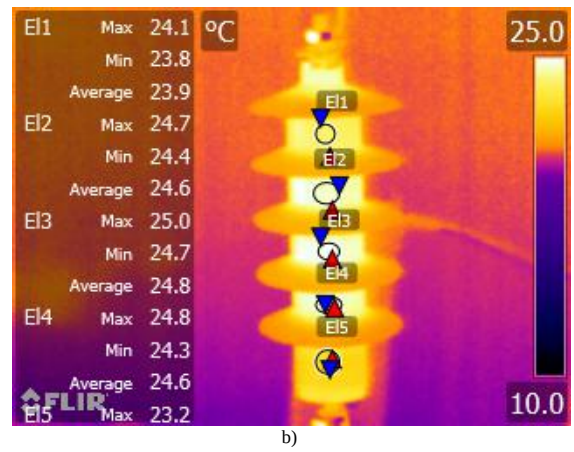

b)

Fig. 6. Thermograms of MOA arresters after 5 minutes under U=18 kV (group B), a) the hot spot noticed in the lower part of the arrester: 22.4°C, b) the hot spot noticed in the middle of the arrester: 25.0°C

As it appears from the literature, it is possible to monitor the high voltage MOAs and detect their fault conditions, using a thermal imaging camera. The leakage current I_{arr} then reaches values in the order of $(1…10)^3$ A. Heat losses are large. [15, 16]. The result of the experiment shows that even a slight increase in leakage current (I_{arr} = 0.6 mA) affects the thermal state of MOA and can be detected by means of an IR camera.

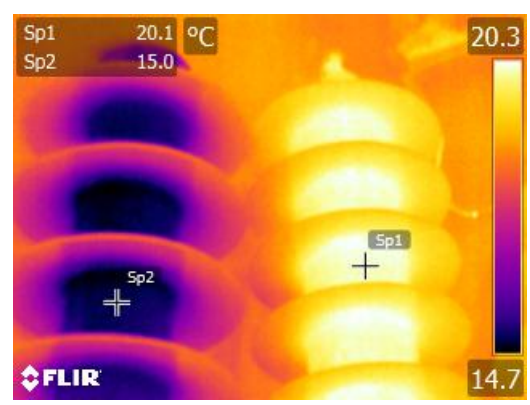

Fig. 7. Thermograms of MOA arresters from group B: one before (left) and one after the experiment (right)

The highest increase in the surface arrester temperature was observed during the first minute (Fig. 8.). The value dT/dt reached 3.05 K/min, SD = 0.46, in group B, where in A group the observed increase was only 0.3 K/min, SD = 2.28. Statistical groups differences dT/dt were important (level of significance α<0.01).

The correlation between the surface temperature and the leakage current, was high; $R = 0.53$.

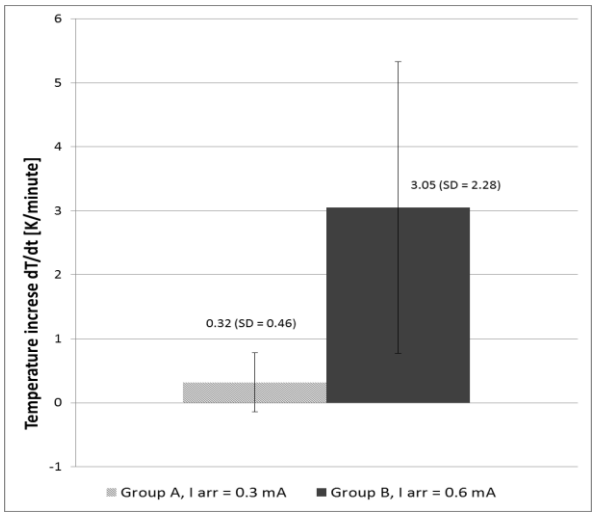

Fig. 8. Surface temperature increase parameter d*T*/d*t*, for surge arresters with different leakage current

4. Conclusions

The surface temperature of the medium voltage surge arrester correlates with an increase in leakage current.

The result shows that the 0.6 mA AC leakage current in the medium voltage metal–oxide surge arrester (18 kV) is above the stable operating point, and the loss of electrical power is higher than the effective heat dissipation in the arrester.

After 5 minutes of high voltage impact $U = 18$ kV, the surface temperature of the MOA surge arrester was (4.32±0.55) K higher than the initial temperature.

The IR camera can be used to detect the faults of ZnO metal – oxide surge arresters that lead to an increase in surface temperature.

Special thanks to the TAURON Dystrybucja company for allowing the research to be carried out.

5. References

[1] Więcek B., DeMey G.: Termowizja w podczerwieni. Podstawy i zastosowania. PAK, Warszawa, 2011.
[2] Lisowska-Lis A.: Thermographic monitoring of the power transformers. Measurement Automation Monitoring, vol. 63(4), pp:154-157, 2017.
[3] ISO 18434-1:2008. Condition monitoring and diagnostics of machines. Thermography.
[4] ASTM E1934-99a(2014), Standard Guide for Examining Electrical and Mechanical Equipment with Infrared Thermography. ASTM International, West Conshohocken, PA, 2014, www.astm.org.
[5] Hinrichsen V.: Metal Oxide Surge Arresters in High Voltage Power Systems – Fundamentals. Siemens A.G., Berlin, 2012. https://assets.new.siemens.com/siemens/assets/public.0.64a37729c7408df1e15b39ca8c9cde8b957a5463.e50001-g630-h197-x-4a00-ableiterhandbuch-teil-1-a4.pdf
[6] Medium voltage surge arresters – product guide. Siemens A.G., Berlin, 2017.
[7] ABB Technical information. Physical properties of zinc oxide varistors, ed. 4, 2002.
[8] Spaeck-Leigsnering Y., Gjonaj E., De Gersem H., Weiland T., Gießel M., Hinrichsen V.: Investigation of thermal stability for a station class surge arrester. IEEE Journal on Multiscale and Multiphysics Computational Techniques 2016, vol 1. DOI: 10.1109/JMMCT.2016.2636250
[9] Zydroń P., Bonk M., Fuśnik Ł., Szafrania B.: Wpływ temperatury na parametry warystorów tlenkowych ograniczników przepięć niskiego napięcia badanych metodami spektroskopii impedancyjnej. Przegląd Elektrotechniczny no. 10, pp:158-162. 2016. DOI: 10.15 199/48.2016.10.38.
[10] Więcek B., De Mey G., Strąkowska M., Chatziathanasiou V., Gmyrek Z., Strzelecki M., Chatzipanagiotou P.: Various applications of complex thermal impedance for transient and AC heat transfer analysis. MAM no. 06 pp:210-214, 2015. http://www.pak.info.pl/index.php?menu=artykulSzczegol&idArtykul=4351
[11] Seyyedbarzegar S. M., Mirzaie M.: Thermal balance diagram modelling of surge arrester for thermal stability analysis considering ZnO varistor degradation effect. IET Generation, Transmission & Distribution; Vol. 10, Iss.: 7, 5 5, 2016. DOI: 10.1049/iet-gtd.2015.0728
[12] Zheng Z., Boggs S. A., Imai T., Nishiwaki S.: Computation of arrester thermal stability. IEEE Trans. Power Deliv., no. 3 vol.25, pp:1526–1529, 2010, . DOI:10.1109/TPWRD.2010.2049163.
[13] Spaeck-Leigsnering Y., Gjonaj E., De Gersem H., Weiland T., Giessely M., Hinrichseny V.: Multi-Rate Time Integration for Coupled Electrical and Thermal Modeling of Surge Arresters. Conference: 2015 Int. Conference on Electromagnetics in Advanced Applications (ICEAA), DOI: 10.1109/ICEAA.2015.7297116.
[14] Chen X., Tian X., Li F.: Research of infrared diagnosed of faults of arrester. 2008 International Conference on High Voltage Engineering and Application, Chongqing, China, November 9-13, 2008.
[15] Srisukkho Ch., Jirapong P.: Analysis of electrical and thermal characteristics of gapless metal oxide arresters using thermal images. The 8th Electrical Engineering/ Electronics, Computer, Telecommunications and Information Technology (ECTI) Association of Thailand - Conference 2011.
[16] Novizon N., Abdul-Malek Z.: Electrical and temperature correlation to monitor fault condition of ZnO surge arrester. 2016. Proc. of 3rd Int. Conf. on Information Tech., Computer, and Electrical Engineering (ICITACEE), Oct 19-21st, 2016, Semarang, Indonesia. pp:182-186. 2016.
[17] Aparaty i układy probiercze średnich i wysokich napięć. ZWAR. 2018. https://docplayer.pl/57421499-Tradycja-dla-nowoczesnosci-aparaty-i-uklady-probiercze-srednich-i-wysokich-napiec.html

Received: 12.12.2018 *Paper reviewed* *Accepted: 04.02.2019*

Agnieszka LISOWSKA-LIS, PhD, eng.

She received PhD in Agriculture Sciences (Ecology) from Agriculture University in Krakow in 2001, and MSc in Electrical Engineering (Electrical Power Engineering) from AGH University of Science and Technology in 2013. Since 2001 she has been working at the State Higher Professional School in Tarnow (PWSZ Tarnow) in the Electrical Engineering Department. She has done research in new measurement techniques, thermovision, ecological aspect in electrical engineering, balanced energy.

e-mail: lisowskalis@pwsztar.edu.pl